

The Effect of Ligand Denticity in Size-Selective Synthesis of Calix[*n*]arene-Stabilized Gold Nanoparticles: A Multitechnique Approach

Luca Pescatori,^[a] Alice Boccia,^[b] Flavio Ciesa,^[a] Francesca Rossi,^[c] Vincenzo Grillo,^[c, d] Arturo Arduini,^[a] Andrea Pochini,^[a] Robertino Zanoni,^{*, [b]} and Andrea Secchi^{*, [a]}

Abstract: A series of gold nanoparticles (AuNPs) stabilized by monodentate, bidentate, and tridentate thiolate calix[*n*]arene ligands **1–3** was prepared by using the Brust–Schiffrin two-phase direct synthesis and characterized with NMR spectroscopy, elemental analysis, transmission electron microscopy (TEM), and X-ray photoelectron spec-

troscopy (XPS). The experimental data show that the particular multidentate structure of calix[*n*]arene derivatives **2** and **3** introduces a control element in the preparation of the gold nanoparti-

cles that allows, in the particular experimental conditions here reported, to obtain very small (≈ 1 nm) AuNPs. These are the first experimental findings that identify a role of ligand “denticity” in the determination of the nuclearity of nanoparticles.

Keywords: calixarenes • denticity • gold • ligand effects • nanoparticles

Introduction

Ligand-stabilized nanoparticles (NPs)^[1] represent an emerging class of organic–inorganic hybrid materials.^[2] Unlike colloids of noble-metal nanoparticles,^[1d,3] these species are constituted by a discrete aggregate of metal atoms stabilized by a shell of organic molecules (arranged like a monolayer around the metal surface) that maintain their stability in solution and prevent aggregation phenomena. Among the plethora of ligand-stabilized nanoparticles synthesized so far,

those characterized by a core of gold atoms and stabilized with a layer of thiolate ligands have attracted the largest interest of the scientific community because of their facile preparation, stability, and solubility in both aprotic and protic solvents.^[4]

A very attractive topological property of ligand-stabilized NPs is the possibility to anchor onto the metallic core a discrete number of suitable receptors in a radial tridimensional arrangement.^[5] In this context, we have shown that AuNPs stabilized with thiolate calix[4]arene ligands can be successfully employed as multivalent hosts for the recognition of organic salts both in organic^[6] and aqueous media.^[7] Another aspect of potentially great importance is associated with quantum size effects that arise from the confinement of electrons in very small objects (≈ 1 nm). Despite the documented potentiality of these systems,^[8] the development of reliable direct synthetic protocols for the synthesis of stable and lipophilic AuNPs characterized both by very small core diameter and potential recognition properties of the organic shell still remains a challenging task.^[9] The combination of these features could indeed lead to the manufacture of nanoscale devices with potential applications as sensors, switches, and new materials that have tunable properties.^[4,5,10]

The synthesis of lipophilic AuNPs is usually obtained through the reduction of aurate salts in the presence of a thiolate ligand. The formation of the stabilized nanoparticles could be considered the result of two competitive processes: growth of the metallic core and gold surface passivation due

[a] Dr. L. Pescatori, Dr. F. Ciesa, Prof. A. Arduini, Prof. A. Pochini, Dr. A. Secchi
Dipartimento di Chimica Organica e Industriale
and Unità INSTM Sez. 4 – UdR Parma, Università di Parma
viale Usberti 17/a, 43124 Parma (Italy)
Fax: (+39)0521-905472
E-mail: andrea.secchi@unipr.it

[b] A. Boccia, Prof. R. Zanoni
Dipartimento di Chimica
Università degli Studi di Roma ‘La Sapienza’
p.le Aldo Moro 5, 00185 Roma (Italy)
Fax: (+39)06490324
E-mail: robertino.zanoni@uniroma1.it

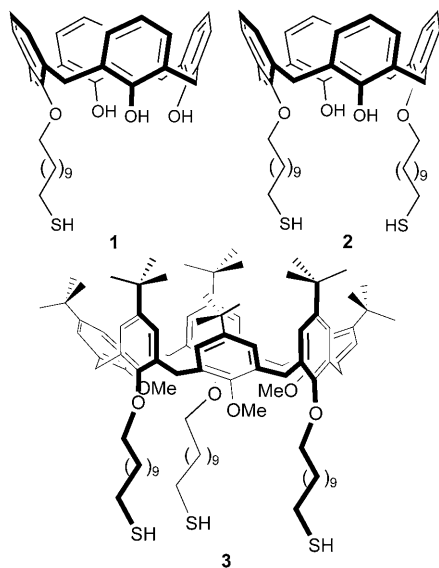
[c] Dr. F. Rossi, Dr. V. Grillo
IMEM-CNR, viale Usberti 37/A, 43124 Parma (Italy)

[d] Dr. V. Grillo
Centro S3, CNR-Istituto Nanoscienze
via Campi 213/A, 41125 Modena (Italy)

Supporting information for this article is available on the WWW under <http://dx.doi.org/10.1002/chem.201001039>.

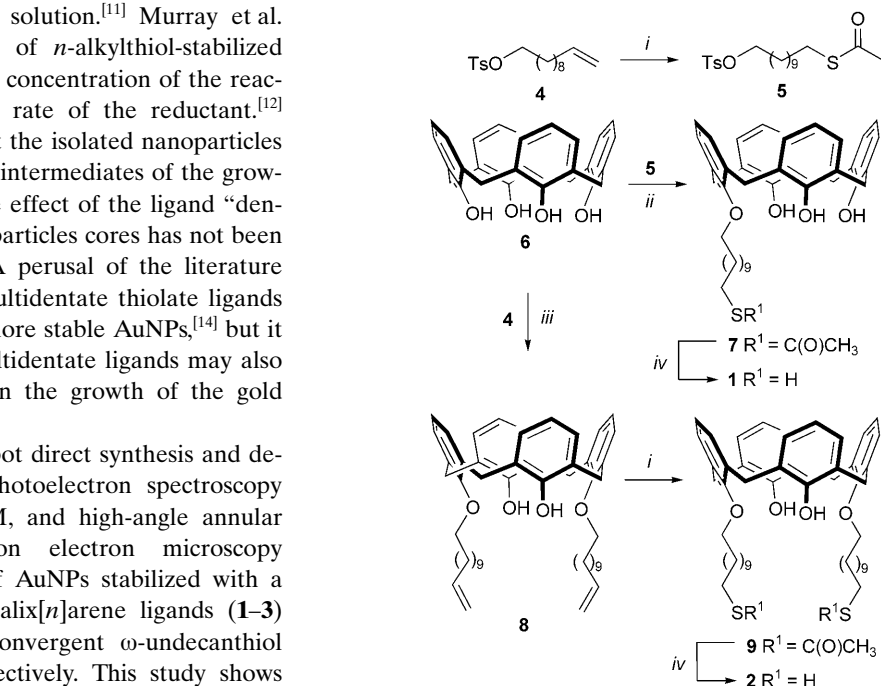
to the presence of the thiols in solution.^[11] Murray et al. have shown that the core size of *n*-alkylthiol-stabilized AuNPs is strongly affected by the concentration of the reactants, temperature, and addition rate of the reductant.^[12] Tsukuda et al. later proposed that the isolated nanoparticles correspond to kinetically trapped intermediates of the growing gold core.^[13] Nevertheless, the effect of the ligand “denticity” on the growth of the nanoparticles cores has not been systematically investigated yet. A perusal of the literature data only offers evidence that multidentate thiolate ligands can promote the preparation of more stable AuNPs,^[14] but it could be also envisioned that multidentate ligands may also exert a relevant kinetic effect on the growth of the gold core.

In this paper we report a one-pot direct synthesis and detailed characterization (X-ray photoelectron spectroscopy (XPS), NMR spectroscopy, TEM, and high-angle annular dark-field scanning transmission electron microscopy (HAADF-STEM)) of a series of AuNPs stabilized with a series of multipodand thiolate calix[*n*]arene ligands (**1–3**) that bear one, two, or three convergent ω-undecanthiol chains on their lower rim, respectively. This study shows that the “ligand denticity” represents a size-control element in the synthesis of these new NPs.



Results and Discussion

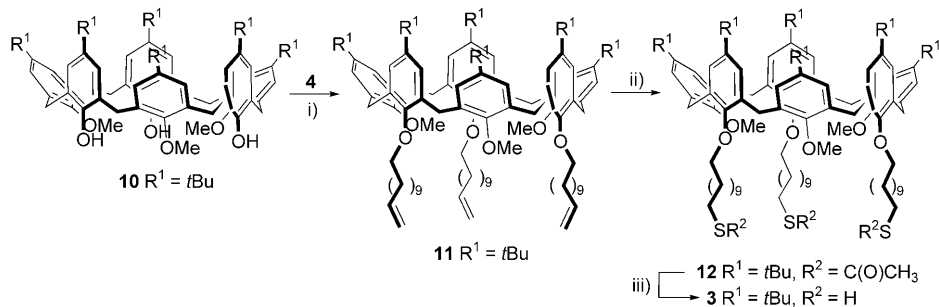
Synthesis of the thiolate calixarene ligands: The thiolate calix[*n*]arene ligands (**1–3**) were synthesized according to Schemes 1 and 2 and fully characterized. The use of thiol groups (SH) as the macrocycle anchoring point on the gold surface was dictated by previous observations that



Scheme 1. Reactions and conditions: i) CH_3COSH , AIBN, toluene, reflux, 5 h; ii) K_2CO_3 , acetone, reflux, 48 h; iii) K_2CO_3 , KI, CH_3CN , reflux, 96 h; iv) 10% HCl, THF/water, reflux, 48 h.

such functions yield RS–Au interactions more stable than those formed by thioether functions ($\text{R}_2\text{S–Au}$).^[15] The calix[*n*]arene macrocycle is known for its large synthetic versatility,^[16] and both rims of these molecular platforms might in principle be used for the insertion of convergent thiol functionalities.^[17] However, the lower rim functionalization offers several advantages. First, the calixarene aromatic cavities, which represent potential recognition units, are exposed to the bulk and not toward the surface. Second, the position of the recognition units with respect to the gold surface can be modulated by using thiolate alkyl chains of variable length.

The thiolate calix[4]arene ligands **1** and **2** that bear one or two convergent ω-undecanthiol chains,^[18] respectively, were synthesized by exploiting the different acidity of the calix[4]-arene phenolic OH groups, which allows the regiochemical



Scheme 2. Reactions and conditions: i) K_2CO_3 , CH_3CN , reflux, 96 h; ii) CH_3COSH , AIBN, toluene, reflux, 5 h; iii) 10% HCl, THF/water, reflux, 48 h.

insertion of a variable number (up to 4) of alkyl chains.^[19] This was accomplished by varying the nature of the base employed during the alkylation process (K_2CO_3) and by choosing the appropriate molar ratio between the calix[4]arene and the alkylating agent. In **1** the sulfur anchoring group was inserted in the alkyl chain before the alkylation of the macrocycle lower rim (see Scheme 1). In particular, undec-10-enyl 4-methylbenzenesulfonate (**4**) was reacted with thioacetic acid in presence of the radical initiator azobisisobutyronitrile (AIBN). The resulting *S*-11-(tosyloxy)undecyl ethanethioate (**5**) was used for the regioselective alkylation of the lower rim of calix[4]arene **6**. Using 0.8 equiv of both the base (K_2CO_3) and of tosylate **5** in dry acetone heated to reflux, the monoalkylated calix[4]arene **7** was obtained in 80% yield. The final acid-catalyzed hydrolysis of the thioester group afforded the monodentate ligand **1** in 72% overall yield. The synthesis of the bidentate ligand **2** was accomplished by reacting calix[4]arene **6** with 2 equiv of undec-10-enyl 4-methylbenzenesulfonate (**4**) in acetonitrile using K_2CO_3 as the base. The thioacetyl group was then inserted in the terminal position of the two ω -undecenyl chains present on the lower rim of **8** through an anti-Markovnikov addition of thioacetic acid. As seen for **1**, the acid-catalyzed hydrolysis of the resulting thioacetyl groups afforded the target bidentate ligand **2** in 44% overall yield.

The “tridentate” thiolate calix[6]arene ligand **3** was prepared in 37% overall yield by using the same synthetic strategy previously adopted for **2**, but with the trimethoxy calix[6]arene **10**, which has the proper symmetry, as starting compound (see Scheme 2).

The 1H NMR spectrum of **2**, taken in $CDCl_3$ (see the Supporting Information), shows a singlet for the two OH protons at $\delta = 8.29$ ppm. The methylene bridges of the macrocycle give rise to a unique AB system of two doublets ($\delta = 4.40$ and 3.45 ppm) for the axial and equatorial protons, respectively. This pattern of signals is typical for a calix[4]arene macrocycle that adopts a cone conformation in solution and confirms that the two ω -undecanthiol chains are oriented on the same side of the macrocycle. The methylene protons in a position α to the SH group are visible as a quartet that integrates four protons at $\delta = 2.59$ ppm. The signal of the SH protons is totally hidden by the strong absorption of the aliphatic protons of the two alkyl chains. To verify the presence of this resonance, the solution of $CDCl_3$ and **2** was submitted to a 2D COSY NMR spectroscopy experiment. In the corresponding 2D spectrum, two relevant symmetric cross-peaks are indeed present; they show the coupling between the quartet assigned to the methylene protons adjacent to the SH group and the resonance of the latter that is found at $\delta \approx 1.4$ ppm (see the Supporting Information).

The 1H NMR spectrum in $CDCl_3$ of monodentate **1** is characterized by a complicated pattern of signals due the absence of symmetry elements in the structure of this ligand (see the Supporting Information). Nevertheless, the monofunctionalization of the lower rim was confirmed by the presence in the spectrum of two singlets at $\delta = 9.74$ and 9.43 ppm in an integral ratio of 1:2 assigned to three OH

protons that are not magnetically equivalent. The three AB systems in 1:2:1 integral ratios that arise from the bridging methylene groups finally confirmed that **1** also adopts a cone conformation on the NMR spectroscopic timescale. As seen for **2**, the methylene group in a position α to SH gives rise to a quartet signal that integrates two protons centered at $\delta = 2.51$ ppm. The 1H NMR spectrum of **3** taken in $CDCl_3$ (see the Supporting Information) shows two singlets, each integrating six protons, at $\delta = 7.28$ and 6.64 ppm for the protons of the differently substituted phenolic rings. The presence of an AB system of two doublets for the axial and equatorial protons of the methylene bridging units at $\delta = 4.58$ and 3.40 ppm, respectively, together with a broad singlet at $\delta \approx 2.2$ ppm suggested that in $CDCl_3$ the calix[6]arene macrocycle predominantly assumes a flattened cone conformation on the NMR spectroscopic timescale. As seen in other studies,^[20] in this conformation the macrocycle possesses three methylated phenolic rings bent and oriented inward with the methoxy groups towards the cavity, whereas those bearing the ω -undecanthiol chains are almost parallel (see Scheme 2).

Synthesis of the calixarene-stabilized AuNPs: A series of calixarene-stabilized AuNPs was prepared by adopting the two-phase method reported by Brust–Schiffrin.^[21] To disclose the role of the ligand denticity on the size dispersion of the resulting coated NPs, we took advantage of the seminal paper published by Murray for *n*-dodecanthiol-stabilized AuNPs (see the Experimental Section).^[12c] In particular, three sets of nanoparticles were prepared for each calixarene ligand (**1–3**) by using different S/Au ratios (3:1, 1:3, and 1:6; see Table 1) in the reaction mixtures. In these ratios, S

Table 1. Composition and mean core size of the calixarene-stabilized AuNPs.

Entry	NP designation	Ligand/ AuCl ₄ [−] molar ratio	S/Au (theor) ^[a]	S/Au (exptl) ^[b]	Organic fraction [%] ^[c]	<i>d</i> _{TEM} [nm] ^[d]
1	C _x S ₁ /Au (1s)	3:1	3:1	0.45	60	(1.5±0.3)
2	C _x S ₁ /Au (1m)	1:3	1:3	0.18	37	(2.2±0.6)
3	C _x S ₁ /Au (1l)	1:6	1:6	0.16	25	(3±1)
4	C _x S ₂ /Au (2s)	1.5:1	3:1	0.88	64	(1.0±0.3)
5	C _x S ₂ /Au (2m)	1:6	1:3	0.37	46	(1.6±0.4)
6	C _x S ₂ /Au (2l)	1:12	1:6	0.2	28	(2.5±0.7)
7	C _x S ₃ /Au (3s)	1:1	3:1	1.09	77	(1.0±0.2)
8	C _x S ₃ /Au (3m)	1:9	1:3	0.38	50	(2.0±0.5)
9	C _x S ₃ /Au (3l)	1:18	1:6	0.18	32	(2.6±0.7)

[a] Equivalents of alkylthiol chains per aurate. [b] Determined through elemental analysis. [c] Determined through TGA or elemental analysis. [d] Determined through TEM measurements (mean ± standard deviation).

expresses the equivalents of thiolate alkyl chains present in solution regardless of the nature of the multidentate ligand. In this way, the outcomes of the synthesis carried out using the same S/Au ratio become independent of the absolute amount of the calixarene employed (see Table 1) and, most importantly, are directly comparable with the literature data relative to monodentate thiolate ligands.

After precipitation from their reaction mixture, all the batches of the isolated NPs were contaminated with both tetraoctylammonium bromide (TOABr), used during the reaction as phase-transfer catalyst, and unreacted calixarene ligand. To have reproducible results, a purification procedure was devised. The black powder of the nanoparticles obtained after the precipitation with ethanol was suspended in a 5:1 mixture of ethanol and dichloromethane, sonicated, and centrifuged at 14000 rpm for at least 20 min. This purification cycle was repeated until no free calixarene ligand was detected (by TLC) in the supernatant solution. The effectiveness of this purification method has been verified through elemental analysis and ^1H NMR spectroscopic measurements (vide infra). The small nanoparticles prepared with a large excess amount of the calixarene ligand (S/Au = 3:1) suffered, as expected by an important contamination of the free ligand. Their purification required a further chromatographic step with a 9:1 mixture of dichloromethane/methanol as eluent.

Characterization of AuNPs: The core-size distribution of the nine sets of synthesized AuNPs was determined through TEM measurements (see Table 1). Each set of nanoparticles was designated as $\text{Cx}_m\text{S}_n/\text{Au}$ (nc), in which m (4 or 6) and n (1 to 3) identify the calixarene macrocycle and its “denticity,” respectively. To distinguish among nanoparticles stabilized with the same ligand but prepared using different S/Au ratios, the index c (s , m , or l) was used. This index would represent the relative core size (s =small, m =medium, or l =large) of the nanoparticles with respect to the 3:1, 1:3, and 1:6 S/Au molar ratio used for their syntheses (vide supra). The analysis of the TEM images showed that for each ligand used, regardless of its denticity, the mean core size (d_{TEM}) of the corresponding nanoparticles was inversely proportional to the S/Au ratio employed during the synthesis (see entries 1–3, 4–6, and 7–9 in Table 1). This was an expected result since the effect of the ligand concentration on the size of the resulting nanoparticles has been already verified.^[12]

More interesting results were obtained by comparing the TEM images taken from the three sets of nanoparticles **1s**, **2s**, and **3s**, which were prepared using an identical S/Au ratio of 3:1, but with the monodentate **1**, the bidentate **2**, and the tridentate **3** calixarene as protecting thiolate ligand, respectively (see Figure 1a–c). The core-size distribution diagrams that correspond to each TEM image clearly show that the nanoparticles present in samples **2s** and **3s** are endowed with a mean core size ($d_{\text{TEM}} \approx 1$ nm; see Figure 1b and c) smaller than those present in **1s** ($d_{\text{TEM}} \approx 1.5$ nm; see Figure 1a).

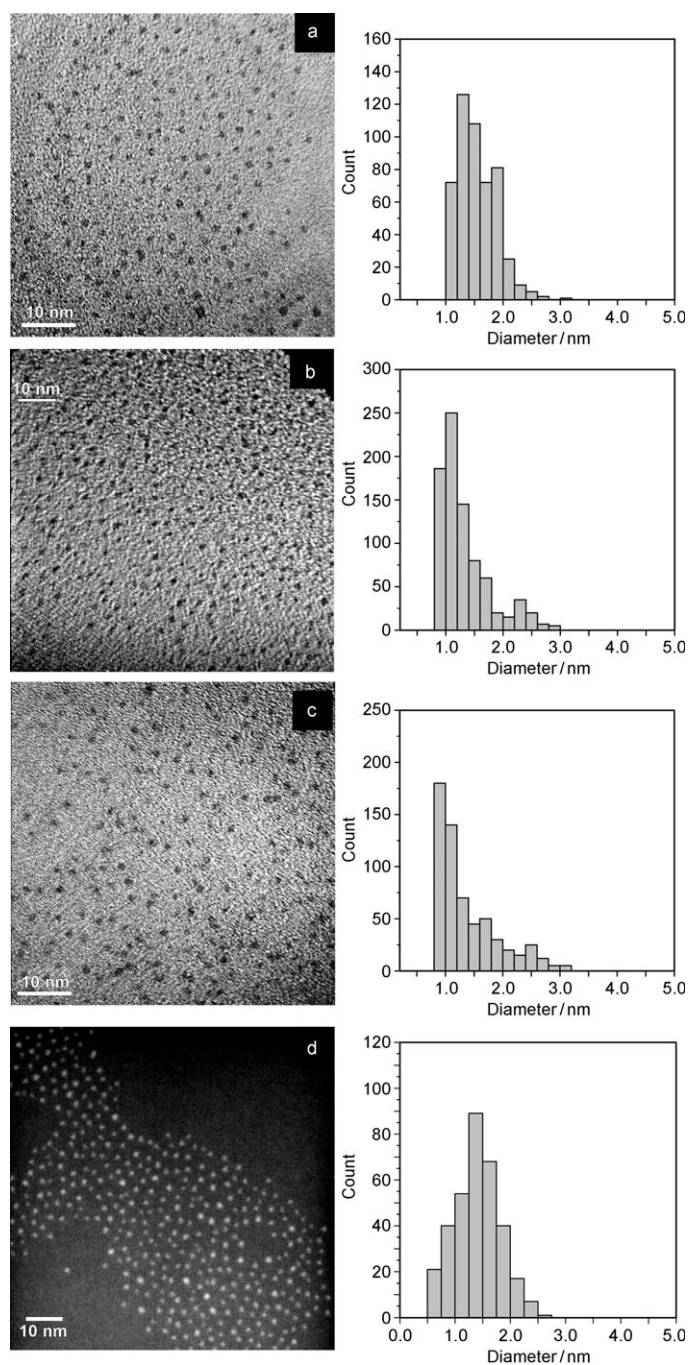


Figure 1. TEM images and core-size distribution diagrams of calixarene-stabilized AuNPs prepared using an S/Au ratio of 3:1. a) **1s** ($d_{\text{TEM}} = (1.5 \pm 0.3)$ nm, $N = 550$); b) **2s** ($d_{\text{TEM}} = (1.0 \pm 0.3)$ nm, $N = 800$); and c) **3s** ($d_{\text{TEM}} = (1.0 \pm 0.2)$ nm, $N = 690$). d) HAADF-STEM image and core-size distribution diagram of **2s** ($d_{\text{STEM}} = (1.2 \pm 0.3)$ nm, $N = 270$). The image was acquired at $1.5\times$ magnification, with an image size of 1024×1024 pixels (pixel dimension = 0.86 \AA).

We propose that the observed reduction in the core size of the nanoparticles stabilized with the multidentate ligands **2** and **3** is due to a convergent arrangement of the (two or three for **2** or **3**, respectively) thiolate chains to the growing gold core, after the formation of the first Au–S bond, which

increases the passivation rate.^[22] In fact, a constant S/Au stoichiometric ratio of 3:1 was chosen in the synthesis of the full series of **1s**, **2s**, **3s** to keep the number of thiol chains constant by adding the proper amount of the ligand (see the effective ligand/AuCl₄⁻ molar ratios of Table 1). This effect was also verified, although to a lesser extent, in the sets of nanoparticles **m** and **l** that were respectively prepared with S/Au ratios of 1:3 and 1:6 (see entries 2, 5, and 8 and 3, 6, and 9, respectively, in Table 1).^[23]

A large relative abundance of NPs in the diameter range 0.9–1.2 nm was found in the **2s** and **3s** samples by TEM measurements, which hints at Au cores mainly composed of 25 to 55 gold atoms.^[24] However, TGA and elemental analyses carried out on **2s** and **3s** revealed a high percentage of organic fraction and experimental S/Au ratios close to one (see Table 1). The latter results suggest that in **2s** and **3s** are also present smaller NPs, such as Au₁₃ covered by six and four calixarene units, respectively.^[25] Since the Au₁₃ nanoclusters are characterized by very small icosahedral gold cores ($d \approx 0.8$ nm), their presence in the **2s** sample was verified through HAADF-STEM analyses.^[26] The Z contrast allows one to clearly distinguish the particles as bright objects on a dark background that corresponds to the light carbon-support film. Statistical analyses of the size of the NPs give a distribution of diameters centered around 1.2 nm, but the presence of subnanometric NPs is confirmed, with the 0.75–1 nm fraction being almost half of the largest fraction, 1.25–1.5 nm (see Figure 1d).

NMR spectroscopic measurements: All the nanoparticles were sufficiently soluble in chloroform to allow for ¹H NMR spectroscopic analysis. In Figure 2, the ¹H NMR spectroscopic stack plot in CDCl₃ (300 MHz) of the NPs **2s**, **2m**, and **2l** along with the “free” calix[4]arene **2** used as the protecting ligand (see the Supporting Information for the NMR spectra of the other NPs) of the NPs is depicted. An overall matching of the resonances present in the spectrum of **2**

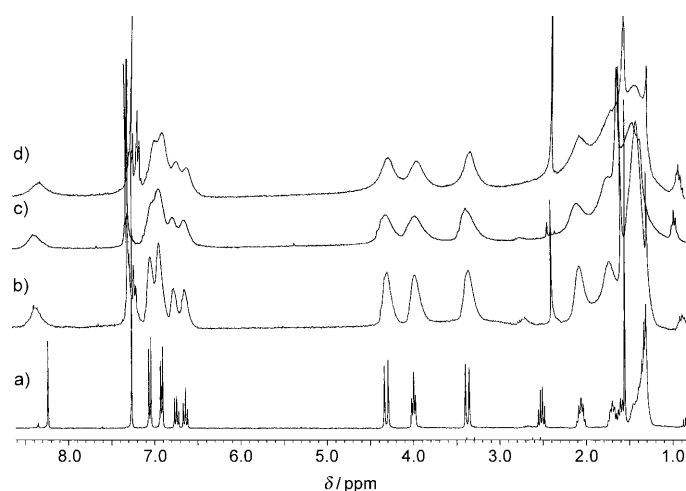


Figure 2. ¹H NMR spectroscopic stack plot (300 MHz, CDCl₃) of a) **2**, b) **2s**, c) **2m**, and d) **2l**.

(see Figure 2d) with those, somewhat broader, present in the spectra of the three nanoparticles shows that the calixarene macrocycle did not undergo significant changes upon introduction onto the gold surface. On the other hand, the broadness of the resonances of the nanoparticles increases on passing from **2s** to **2l**, which is in agreement with previous findings reported in the literature.^[12c] This is due to several concomitant effects: an average arrangement of the calix[4]arene macrocycles around the gold core that reflects the polydispersity of the size of the nanoparticles, and the predictable slow tumbling motion of the NPs in solution that reduces the transverse relaxation time.^[27] As expected, the anchoring process of the thiolate SH groups on the surface of the metal induces the disappearance of the diagnostic signal of the methylene protons of the CH₂ group adjacent to the S atom directly attached to the gold surface, which is visible in the free ligands as a quartet centered at around $\delta = 2.5$ ppm (see Figure 2d).

XPS measurements: An XPS analysis has been conducted on the three series of **s**, **m**, and **l** NPs and on the ligand-exchanged Au₁₁ nanoclusters (**2ex**). The latter nanoparticles were obtained through a ligand-place-exchange reaction by reacting, in CH₂Cl₂, Au₁₁(PPh₃)₇Cl₃ undecagold clusters with an excess amount of thiolate calix[4]arene **2** (see the Experimental Section).^[9c,28] The relevant XPS regions for the investigated systems are those of Au 4f and S 2p, which appear as complex peaks and required curve-fitted components (Figures 3 and 4). As evidenced by a rigid energy shift of the overall spectrum, the nanoparticles experienced static charging under X-rays to different amounts, which were quantified and corrected by taking the distinct energy separations between the C 1s peak components, respectively, due to the graphite tip and the NPs. Such static charging only affected **m** and **s** NPs, to comparable extents.

Theoretically reconstructed Au 4f peaks invariably show three spin-orbit split components (Table 2), whereas two main components were expected, one due to the Au–S bonds and the second to the Au–Au (both central and surface atoms) bonds. Their assignment is further complicated by the fact that the three Au components happen to follow at different binding energies (BEs) depending on the nanoparticles size. We assign the Au electronic states for **l**, **m**, and **s** NPs by first considering the typical energy separation between Au 4f_{7/2} components, as extracted from the relevant literature:^[29] Au–Au^I ((1.3 ± 0.3) eV) and Au^I–Au^{III} ((1.7 ± 0.3) eV). These values are consistently reproduced by peaks Au(a), Au(b), and Au(c) in Table 2, which are present with different relative ratios in the series depending on the mean dimension of NPs. The minor Au(c) component can be assigned to the Au^{III} species that likely derive from AuCl₄⁻. It is expected on the simple basis of the decreasing trend of surface/bulk atomic ratio in a nanoparticle as a function of its increasing nuclearity that the Au(a)/Au(b) ratio is the largest for **l** and the smallest for **s** NPs, as indeed was found, with the **m** ones lying definitely closer to the latter (Figure 3). The main Au 4f_{7/2} component in all the spectra is

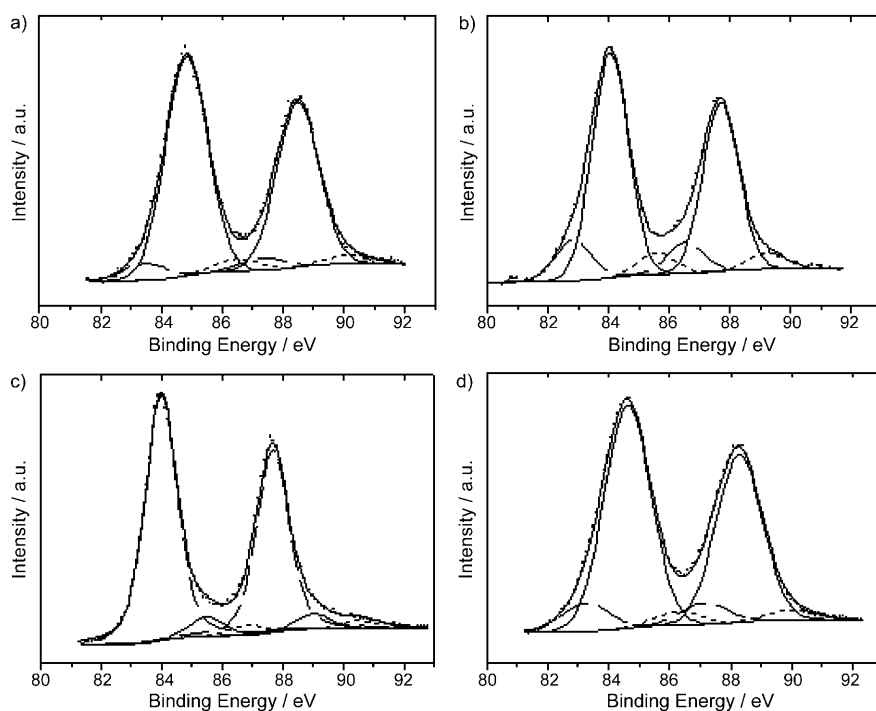


Figure 3. Au 4f XPS spectral regions of a) **2s**, b) **2m**, c) **2l**, and d) **2ex**. Experimental curve (dots) and Au $4f_{7/2,5/2}$ curve-fitted components: Au(a) (dashed line), Au(b) (solid line), and Au(c) (dotted line).

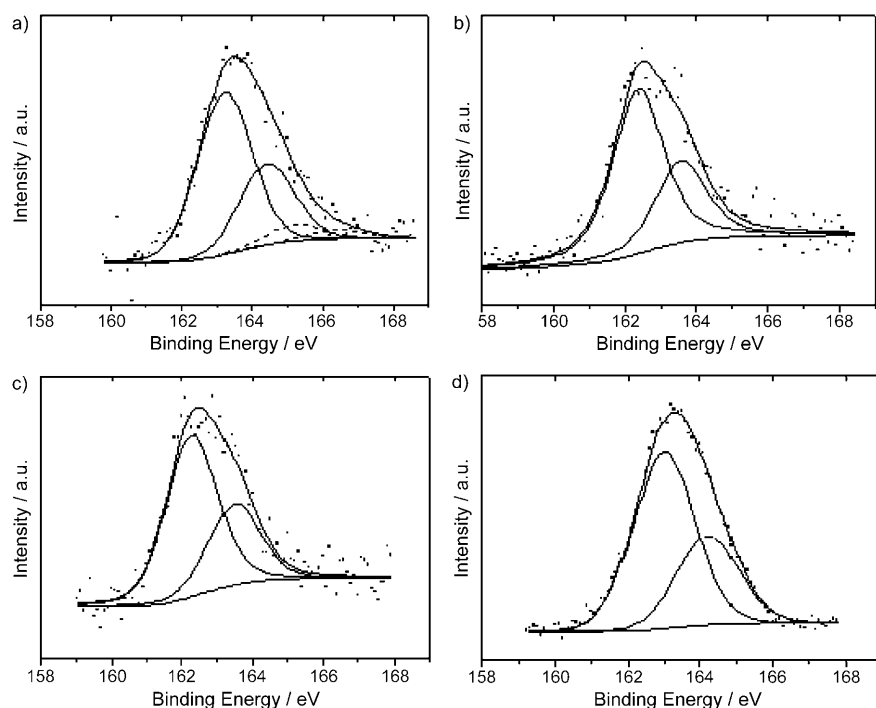


Figure 4. S 2p XPS spectral regions of a) **2s**, b) **2m**, c) **2l**, and d) **2ex**. Experimental curve (dots) and S $2p_{3/2,1/2}$ curve-fitted components: S–Au (solid line), S–S (dotted line).

invariably associated with a relative shift to the main S $2p_{3/2}$ component equal to (78.3 ± 0.1) eV, a value found in the literature as characteristic for S-bound Au atoms.^[29] The S 2p spectra present a major component due to the thiolate–Au

bond, accompanied in the case of *s* NPs by a small contribution from distinct sulfur species. We assign this minor component to disulfide bridges that connect distinct calixarenes,^[30] since NMR spectroscopic analysis excludes the alternative assignment in terms of free thiols, because of the absence of SH groups in the NPs.

Relevant quantitative results (S/Au and Au(b)/Au(a)) are reported in Table 2. We note that the S/Au ratios determined by means of XPS spectroscopy are usually higher than those determined by means of elemental analysis (see Tables 1 and 2), most likely because of the photon attenuation exerted by the ligand shell on the Au core. The S 2p major component due to the thiolate–Au bond is also fully compatible with the structural motif (“staple”) first seen in the external organic shell of the X-ray structure of the Au₂₅ nanoparticles stabilized with phenylethanethiolate groups reported by Murray^[24b] and confirmed in subsequent reports.^[31] We note that Au BEs and relative quantitative ratios for **2ex** are closely comparable to **2s** and **3s**, and distinct from **2m**, **2l**, and **1s**. More in detail, the S/Au and A(b)/Au(a) ratios obtained for **2ex**, and expected for an Au₁₁ cluster, are only reproduced in the cases of **2s** and **3s**, within the experimental error.

As for BEs, Au(a) $4f_{7/2}$ values for *s* and *m* NPs fall in the range of 82.8–83.5 eV, that is, at consistently negative BE shift with respect to bulk Au (84.0 eV). Their interpretation in terms of a negatively charged Au central atom is supported by previous literature reports.^[32] We can take the relative abundance

of Au(a) together with S/Au ratios as an indirect measure of the nuclearity of the nanoparticles, thus allowing for a distinction to be made between *s*, *m*, and *l*. In fact, the experimental S/Au and Au(b)/Au(a) ratios are inversely pro-

Table 2. XPS binding energies for Au 4f and S 2p and relative quantitative ratios for different series of calixarene-stabilized AuNPs.

Entry	NP designation	Au 4f _{7/2}		S 2p _{3/2}		S/Au (XPS) ^[a]	Au(b)/Au(a) ^[a]	d _{TEM} [nm] ^[b]
		Label	BE [eV]	Label	BE [eV]			
1	Cx ₄ S ₁ /Au (1s)	Au(a)	82.9	S–Au	162.9	0.7	6	(1.5±0.3)
		Au(b)	84.7					
		Au(c)	86.7					
2	Cx ₄ S ₂ /Au (2ex)	Au(a)	83.3	S–Au	163.0	1.0	8	[c]
		Au(b)	84.6					
		Au(c)	87.1					
3	Cx ₄ S ₂ /Au (2s)	Au(a)	83.5	S–Au	163.2	1.0	10 ^[d]	(1.0±0.3)
		Au(b)	84.8	S–S	165.3			
		Au(c)	86.5					
4	Cx ₄ S ₂ /Au (2m)	Au(a)	82.8	S–Au	162.4	0.6	5	(1.6±0.4)
		Au(b)	84.1					
		Au(c)	85.6					
5	Cx ₄ S ₂ /Au (2I)	Au(a)	84.0	S–Au	162.3	0.3	0.1	(2.5±0.7)
		Au(b)	85.5					
		Au(c)	86.8					
6	Cx ₆ S ₃ /Au (3s)	Au(a)	82.8	S–Au	162.3	1.5	9	(1.0±0.2)
		Au(b)	84.1	S–S	163.6			
		Au(c)	85.4					

[a] Quantitative ratios (associated uncertainty of ±10%). [b] From Table 1, reported for clarity. [c] Not determined. [d] Average value calculated from different **2s** batches.

portional to the size of the nanoparticles. This trend is consistent with the observation that the smaller the core size of the NPs, the larger the percentage of surface Au atoms bound to S. In addition to that, we could tentatively infer the nuclearity of the NPs by comparing the present results with the expected values in the notable cases of previously reported Au₁₁, Au₁₃, Au₂₅(SR)₁₈[−], Au₃₈/Au₄₀, Au₅₅, Au₆₈, Au₁₀₂, and Au₁₄₄ clusters.^[31a]

On the basis of the data in Table 2 on the S/Au and Au(b)/Au(a) ratios, the nuclearities of **2s** and **3s** are both likely assigned to Au₁₁ or Au₁₃ (which can be hardly distinguished by XPS only), whereas **2m** NPs belong to higher-nuclearity species. As regards to **2I**, the S/Au and Au(b)/Au(a) ratios are too small to find a correspondence with the above range of Au nuclearity, thus hinting at a larger range of nanoparticle diameters. We also note that, in the case of **2I**, although TEM measurements clearly distinguish a larger average dimension of the particles, XPS results are distinct from the analogous **s** and **m**, but they could be mainly related to the outer shell of the particle, since its experimental diameter range becomes comparable to the inelastic mean free path for Au 4f photoelectrons at the photon energy applied here.

Conclusion

In summary, the synthesis and characterization of a series of AuNPs stabilized with calixarene derivatives functionalized with alkylthiol chains on their lower rim has been reported. The group of experimental results that have emerged from the different techniques adopted here constitutes a sound basis to demonstrate that, by making use of suitable calixarenes, a full series of AuNPs of different sizes can be ob-

tained, and that ligand denticity can play a role in addressing the synthetic outcomes towards the nanodimensional range.^[33] In fact: 1) the mean diameters calculated for the NPs stabilized with the monodentate calix[4]arene ligand **1** (**1s**, **1m**, and **1I**) are always larger than those calculated for the NPs loaded with the bidentate **2** and tridentate **3** thiolate calixarene ligands that were obtained using the same experimental conditions and the same equivalents of thiolate alkyl chains present in solution. The TEM measurements also show that the diameter of the NPs present in the samples **1s**, **1m**, and **1I** is comparable, in terms of mean diameter and size distribution, to those of NPs prepared by

Murray from the monodentate dodecanthiol ligand under similar experimental conditions.^[12c] 2) XPS results support a distinct size for sample **1s** with respect to **2s** and **3s** (the latter two being closely comparable). Actually, the positions in energy of Au 4f peak components, and their relative quantitative ratios, are clearly distinct in the two subsets, and can be interpreted in the light of the literature as size-dependent effects. 3) Elementary analysis of the **2s** and **3s** samples shows the presence of NPs with nuclearities around 1 nm.

These results open new possibilities for the synthesis of NPs that merge the high potential of calix[n]arene receptors with those associated to quantum size effects. Studies are undergoing in our laboratory to apply these achievements in the preparation of working devices.

Experimental Section

Chemicals: All reactions were carried out under nitrogen; all solvents were freshly distilled under nitrogen and stored over molecular sieves for at least 3 h prior to use. ¹H and ¹³C NMR spectra were recorded using instruments operating at 300 and 75 MHz, respectively. Mass spectra were recorded in ESI mode. Melting points are uncorrected. Undec-10-enyl 4-methylbenzenesulfonate **4**,^[34] calix[4]arene **6**,^[35] 38,40,42-trimethoxy-*p*-tert-butylcalix[6]arene **10**,^[36] and AuPPh₃Cl^[37] were prepared according to published procedures.

Synthesis of the thiolate calix[4]arene ligands

Thioate 5: A tip of a spatula of AIBN was added to a solution of tosylate **4** (5 g, 15.4 mmol) and thioacetic acid (5.9 g, 77 mmol) in dry toluene (200 mL). After heating at reflux for 5 h, the reaction was quenched by addition of water (200 mL). The separated organic phase was dried over Na₂SO₄ and the solvent evaporated to dryness under reduced pressure. The solid residue was purified by column chromatography (silica gel, eluent: hexane/ethyl acetate 9:1) to afford **5** as a yellow low-melting solid (90%). M.p. 28.0–29.5 °C; ¹H NMR (300 MHz, CDCl₃): δ = 7.74 (d, J =

8.3 Hz, 2H), 7.30 (d, $J=8.3$ Hz, 2H), 3.97 (t, $J=6.6$ Hz, 2H), 2.81 (t, $J=7.2$ Hz, 2H), 2.40 (s, 3H), 2.37 (s, 3H), 1.7–1.4 (m, 4H), 1.4–1.1 ppm (m, 14H); ^{13}C NMR (75 MHz, CDCl_3): $\delta=195.0, 144.4, 133.3, 130.5, 128.3, 71.0, 31.0, 29.9, 29.7$ (2 resonances), 29.5, 29.4, 29.3, 29.2 (2 resonances), 25.7, 22.0 ppm; MS (ESI): m/z (%): 347 (100) [$M+\text{Na}$]; elemental analysis calcd (%) for $\text{C}_{20}\text{H}_{32}\text{O}_4\text{S}$: C 59.96, H 8.05, S 16.01; found: C 59.57, H 8.15, S 16.23.

Calix[4]arene 7: A solution of calix[4]arene **6** (0.42 g, 1 mmol), K_2CO_3 (0.11 g, 0.8 mmol), and **5** (0.26 g, 0.8 mmol) in dry acetone (70 mL) was poured into a small glass autoclave filled with nitrogen. After sealing the autoclave, the reaction mixture was heated at reflux at 80°C for 48 h. After this period, the mixture was cooled at room temperature and the solvent evaporated to dryness under reduced pressure. The solid residue was dissolved in a 10% (w/v) aqueous solution of HCl (100 mL) and CH_2Cl_2 (100 mL). The separated organic phase was washed with water up to neutrality, dried over Na_2SO_4 , and evaporated to dryness under reduced pressure. The crude product was purified by column chromatography (silica gel, eluent: *n*-hexane/ CH_2Cl_2 7:3) to afford **7** as a white solid (80%). M.p. 53.0–54.0°C; ^1H NMR (300 MHz, CDCl_3): $\delta=9.75$ (s, 1H), 9.44 (s, 2H), 7.1–7.0 (m, 8H), 6.87 (t, $J=7.5$ Hz, 1H), 6.7–6.6 (m, 3H), 4.37 (d, $J=13$ Hz, 2H), 4.28 (d, $J=14$ Hz, 2H), 4.16 (t, $J=7.2$ Hz, 2H), 3.47 (d, $J=14$ Hz, 2H), 3.46 (d, $J=13$ Hz, 2H), 2.86 (t, $J=7.2$ Hz, 2H), 2.32 (s, 3H), 2.2–2.1 (m, 2H), 1.8–1.6, 1.6–1.5, and 1.5–1.3 ppm (3m, 16H); ^{13}C NMR (75 MHz, CDCl_3): $\delta=196.0, 151.4, 150.8, 149.2, 134.2, 129.2, 128.8, 128.7$ (2 resonances), 128.3, 126.0, 121.9, 120.8, 77.1, 31.8, 31.4, 30.6, 29.8, 29.4 (2 resonances), 29.1, 28.8, 25.8 ppm; MS (ESI): m/z (%): 653 (100) [$M+1$], 675 (50) [$M+\text{Na}$]; elemental analysis calcd (%) for $\text{C}_{41}\text{H}_{48}\text{O}_5\text{S}$: C 75.43, H 7.41, S 4.91; found: C 75.22, H 7.50, S 4.56.

Calix[4]arene 8: A mixture of calix[4]arene **6** (3 g, 7 mmol), K_2CO_3 (2.9 g, 21 mmol), tosylate **4** (7 g, 21 mmol), and KI (cat.) in CH_3CN (150 mL) was stirred and heated under reflux. After four days, the solvent was evaporated under vacuum and the solid residue was dissolved in CH_2Cl_2 . The organic phase was washed with H_2O up to neutrality and dried over Na_2SO_4 . After evaporation of the solvent under reduced pressure, the resulting crude product was purified by column chromatography (silica gel, *n*-hexane/ethyl acetate 9:1) to give **8** as yellowish solid (70%). M.p. 120–122°C; ^1H NMR (300 MHz, CDCl_3): $\delta=8.24$ (s, 2H), 7.05 (d, $J=7$ Hz, 4H), 6.91 (d, $J=7$ Hz, 4H), 6.72 (t, $J=7$ Hz, 2H), 6.62 (t, $J=7$ Hz, 2H), 5.9–5.7 (m, 2H), 5.1–4.9 (m, 4H), 4.32 (d, $J=14$ Hz, 4H), 3.99 (t, $J=6$ Hz, 4H), 3.37 (d, $J=14$ Hz, 4H), 2.2–2.0 (m, 8H), 1.8–1.6 (m, 4H), 1.6–1.2 ppm (m, 20H); ^{13}C NMR (CDCl_3 , 75 MHz): $\delta=155.2, 150.8, 138.0, 132.3, 127.6, 127.2, 127.0, 124.0, 117.7, 112.9, 76.4, 32.6, 30.2, 28.8, 28.4, 28.3, 27.9, 24.8$ ppm; MS (ESI): m/z (%): 729 [$M+H$]; elemental analysis calcd (%) for $\text{C}_{50}\text{H}_{64}\text{O}_4$: C 82.37, H 8.85; found: C 82.45, H 8.52.

Calix[4]arene 9: A catalytic amount of AIBN was added to a solution of calix[4]arene **8** (3 g, 4.2 mmol) and thioacetic acid (1.3 g, 17 mmol) in toluene (100 mL). The resulting homogeneous mixture was heated at reflux for 5 h, then the solvent was evaporated to dryness under reduced pressure. The solid residue was dissolved in CH_2Cl_2 and the organic phase was washed twice with H_2O and with a saturated solution of NaHCO_3 . After the removal of the solvent under reduced pressure, the solid residue was purified by column chromatography (silica gel, *n*-hexane/ethyl acetate 8:2) to afford **9** as a yellowish sticky solid (70%). M.p. 84.5–85.5°C; ^1H NMR (300 MHz, CDCl_3): $\delta=8.23$ (s, 2H), 7.04 (d, $J=7$ Hz, 4H), 6.91 (d, $J=7$ Hz, 4H), 6.73 (t, $J=7$ Hz, 2H), 6.63 (t, $J=7$ Hz, 2H), 4.30 (d, $J=14$ Hz, 4H), 3.99 (t, $J=6$ Hz, 4H), 3.37 (d, $J=14$ Hz, 4H), 2.85 ($J=6$ Hz, 4H), 2.32 (s, 6H), 2.1–2.0 (m, 4H), 1.8–1.7 (m, 4H), 1.6–1.4 ppm (2m, 28H); ^{13}C NMR (75 MHz, CDCl_3): $\delta=153.3, 152.0, 133.4, 128.8, 128.3, 128.1, 125.1, 118.9, 76.6, 31.4, 30.5, 29.9, 29.6, 29.5, 29.4, 29.1, 28.8, 25.9$ ppm; MS (ESI): m/z (%): 904 [$M+\text{Na}$]; elemental analysis calcd (%) for $\text{C}_{54}\text{H}_{62}\text{O}_6\text{S}_2$: C 73.51, H 8.22, S 7.27; found: C 73.55, H 8.14, S 6.98.

Calix[6]arene 11: Tosylate **4** (0.96 g, 3 mmol) was added to a stirred solution of calix[6]arene **10** (1 g, 0.98 mmol) and K_2CO_3 (0.4, 3 mmol) in acetonitrile (200 mL). The resulting heterogeneous mixture was heated at reflux for 4 d. After this period, the solvent was evaporated to dryness under reduced pressure. The solid residue was dissolved in a 10% (w/v) aqueous solution of HCl in water (100 mL) and ethyl acetate (200 mL).

The organic phase was separated, washed with brine up to neutrality, and dried over Na_2SO_4 . After the removal of the solvent under reduced pressure, the solid residue was purified by column chromatography (silica gel, eluent: *n*-hexane/ CH_2Cl_2 8:2) to afford **11** as a white solid (55%). M.p. 133–135°C; ^1H NMR (300 MHz, CDCl_3 , cone conformer): $\delta=7.29$ (s, 6H), 6.64 (s, 6H), 5.9–5.7 (m, 3H), 5.1–4.8 (m, 6H), 4.58 (d, $J=14.1$ Hz, 6H), 3.88 (t, $J=6.4$ Hz, 6H), 3.40 (d, $J=14.1$ Hz, 6H), 2.20 (s, 9H), 2.1–2.0 (m, 6H), 2.0–1.8 (m, 6H), 1.6–1.5 (m, 6H), 1.39 (s, 27H), 1.4–1.3 (m, 30H), 0.79 ppm (s, 27H); ^{13}C NMR (75 MHz, CDCl_3 , cone conformer): $\delta=154.5, 152.1, 145.5, 145.2, 139.2, 133.6, 133.3, 127.9, 123.4, 114.1, 73.0, 60.2, 34.2, 33.9, 33.8, 31.6, 31.3, 31.2, 30.4, 29.7, 29.6, 29.5, 29.1, 28.9, 26.2$ ppm; MS (ESI): m/z (%): 1495 (100) [$M+\text{Na}$]; elemental analysis calcd (%) for $\text{C}_{102}\text{H}_{150}\text{O}_6$: C 83.15, H 10.32; found: C 83.20, H 10.52.

Calix[6]arene 12: A tip of a spatula of AIBN was added to a solution of **11** (1 g, 0.68 mmol) and thioacetic acid (0.37 g, 4.9 mmol) in dry toluene (100 mL). After heating at reflux for 5 h, the reaction was quenched by addition of water (100 mL). The separated organic phase was dried over Na_2SO_4 . After the removal of the solvent under reduced pressure, the solid residue was purified by column chromatography (silica gel, eluent: *n*-hexane/ethyl acetate 95:5) to afford **12** as a white solid (80%). M.p. 125–127°C; ^1H NMR (300 MHz, CDCl_3 , cone conformer): $\delta=7.29$ (s, 6H), 6.66 (s, 6H), 4.59 (d, $J=15.0$ Hz, 6H), 3.88 (t, $J=6.5$ Hz, 6H), 3.40 (d, $J=15.2$ Hz, 6H), 2.87 (t, $J=7.3$ Hz, 6H), 2.32 (s, 9H), 2.22 (s, 9H), 2.0–1.8 (m, 6H), 1.6–1.4 (m, 6H), 1.42 (s, 27H), 1.4–1.1 (m, 42H), 0.80 ppm (s, 27H); ^{13}C NMR (75 MHz, CDCl_3 , cone conformer): $\delta=196.0, 154.4, 152.0, 145.6, 145.2, 133.8, 133.6, 133.2, 127.9, 123.3, 73.0, 60.1, 34.2, 34.0, 33.9, 31.6, 31.4, 31.1, 30.6, 30.4, 29.6, 29.5, 29.4, 29.1, 28.8, 26.3, 26.2$ ppm; MS (ESI): m/z (%): 1723 [$M+\text{Na}$]; elemental analysis calcd (%) for $\text{C}_{108}\text{H}_{162}\text{O}_9\text{S}_3$: C 76.23, H 9.52, S 5.65; found: C 76.35, H 9.43, S 5.81.

General procedure for the removal of the thioacetyl protecting groups:

A solution of the appropriate calix[*n*]arene derivative (1 mmol) in a mixture of THF (20 mL) and HCl (10% w/v in H_2O , 20 mL) was heated at reflux for 48–72 h. After cooling to room temperature, the mixture was extracted with CH_2Cl_2 (30 mL). The resulting organic phase was separated, washed with water up to neutrality, dried over Na_2SO_4 , and evaporated to dryness under reduced pressure.

Calix[4]arene 1: The oily residue obtained from the hydrolysis of **7** was purified by column chromatography (silica gel, eluent: *n*-hexane/ CH_2Cl_2 7:3) to afford **1** as a white solid (90%). M.p. 87.0–88.0°C; ^1H NMR (300 MHz, CDCl_3): $\delta=9.75$ (s, 1H), 9.43 (s, 2H), 7.1–7.0 (m, 8H), 6.87 (t, $J=7.5$ Hz, 1H), 6.7–6.6 (m, 3H), 4.37 (d, $J=13$ Hz, 2H), 4.28 (d, $J=14$ Hz, 2H), 4.15 (t, $J=7.2$ Hz, 2H), 3.47 (d, $J=14$ Hz, 2H), 3.46 (d, $J=13$ Hz, 2H), 2.6–2.5 (m, 2H), 2.2–2.1 (m, 2H), 1.8–1.6, 1.6–1.5, and 1.5–1.3 ppm (3m, 16H); ^{13}C NMR (75 MHz, CDCl_3): $\delta=151.4, 150.8, 149.2, 134.2, 129.3, 128.8, 128.7$ (2 resonances), 128.4, 126.0, 121.9, 120.9, 77.4, 34.0, 31.9, 31.4, 29.9, 29.5 (2 resonances), 29.4, 29.1, 28.4, 25.9, 24.6 ppm; MS (ESI): m/z (%): 611 (10) [$M+1$], 634 (85) [$M+\text{Na}$], 650 (60) [$M+K$]; elemental analysis calcd (%) for $\text{C}_{39}\text{H}_{46}\text{O}_4\text{S}$: C 76.68, H 7.59, S 5.25; found: C 75.62, H 7.46, S 4.81.

Calix[4]arene 2: The oily residue obtained from the hydrolysis of **9** was purified by column chromatography (silica gel, eluent: *n*-hexane/ CH_2Cl_2 7:3) to afford **2** as a white solid (80%). M.p. 300–302°C; ^1H NMR (300 MHz, CDCl_3): $\delta=8.29$ (s, 2H), 7.13 (d, $J=7$ Hz, 4H), 6.96 (d, $J=7$ Hz, 4H), 6.8–6.7 (m, 4H), 4.40 (d, $J=14$ Hz, 4H), 4.07 (t, $J=6$ Hz, 4H), 3.45 (d, $J=14$ Hz, 4H), 2.7–2.5 (m, 4H), 2.2–2.1 (m, 4H), 1.9–1.8 (m, 4H), 1.8–1.7 (m, 4H), 1.6–1.3 ppm (m, 24H); ^{13}C NMR (75 MHz, CDCl_3): $\delta=153.3, 133.4, 128.8, 128.3, 128.1, 125.2, 118.9, 76.7, 34.0, 31.4, 30.0, 29.6, 29.5, 29.4, 29.1, 28.4, 25.9, 24.6$ ppm; ESI (MS): m/z (%): 818 [$M+\text{Na}$]; elemental analysis calcd (%) for $\text{C}_{50}\text{H}_{68}\text{O}_4\text{S}_2$: C 75.33, H 8.60, S 8.05; found: C 75.40, H 8.32, S 8.26.

Calix[6]arene 3: The oily residue obtained from the hydrolysis of **12** was purified by column chromatography (silica gel, eluent: *n*-hexane/ethyl acetate 95:5) to afford **3** as a white solid (85%). M.p. 69.5–70.5°C; ^1H NMR (300 MHz, CDCl_3 , cone conformer): $\delta=7.28$ (s, 6H), 6.64 (s, 6H), 4.58 (d, $J=15.0$ Hz, 6H), 3.88 (t, $J=6.4$ Hz, 6H), 3.40 (d, $J=15.0$ Hz, 6H), 2.51 (q, $J=7.2$ Hz, 6H), 2.20 (s, 9H), 2.0–1.8 (m, 6H), 1.7–

1.2 (m, 81H), 0.79 ppm (s, 27H); ^{13}C NMR (75 MHz, CDCl_3 , cone former): δ = 154.4, 152.0, 145.6, 145.2, 133.6, 133.5, 133.2, 127.9, 123.3, 73.0, 60.1, 34.2, 34.0, 33.9, 31.6, 31.4, 31.3, 31.2, 31.1, 30.6, 30.4, 29.6, 29.53, 29.50, 29.4, 29.0, 28.3, 26.2, 24.6 ppm; ESI (MS): m/z : 1597 [$M+\text{Na}$]; elemental analysis calcd (%) for $\text{C}_{102}\text{H}_{156}\text{O}_6\text{S}_3$: C 77.76, H 9.91, S 6.10; found: C 77.61, H 10.10, S 6.10.

Synthesis of the calixarene-stabilized gold nanoparticles: The calixarene-stabilized nanoparticles were synthesized according to the general procedure published by Murray for *n*-dodecanthiol-stabilized nanoparticles using S/Au ratios of 3:1, 1:3, and 1:6, respectively.^[12c] All the preparations were carried out using $\text{HAuCl}_4 \cdot x\text{H}_2\text{O}$ (1 mmol) as the source of gold, tetrabutylammonium bromide (TOABr; 2.5 mmol) as the transfer catalyst, and NaBH_4 (10 mmol) as the reductant. In each preparation, the amount of the calix[n]arene ligand used (**1–3**) was changed according to the ligand “denticity” to match the requested S/Au ratios. The purification procedure has been changed as follows: after the gold reduction, toluene was evaporated to dryness under reduced pressure and the temperature maintained below 50°C. The black sticky residue obtained was suspended in ethanol (25 mL) and sonicated. The black powder formed was separated by suction filtration and dissolved in a 5:1 ethanol/dichloromethane mixture, sonicated, and centrifuged at 14000 rpm for 20 min. The supernatant solution was eliminated and the solid residue dried under vacuum. The purification cycle was repeated until the free calixarene ligand was no longer detectable by TLC in the supernatant solution. The isolated nanoparticles were characterized by elemental analysis, NMR spectroscopy, TEM, and XPS measurements.

Nanoparticles stabilized with the monodentate calix[4]arene ligand 1

$\text{C}_{x_4}\text{S}_y/\text{Au}$ (**1s**): Complex **1** (1.8 g; 3 mmol corresponding to S/Au 3:1) was used as the gold passivating agent. The solid residue obtained after the centrifugation cycle required a further purification step to eliminate the large excess amount of free **1** that was contaminating the nanoparticles. A chromatographic separation was accomplished using a 9:1 mixture of $\text{CH}_2\text{Cl}_2/\text{CH}_3\text{OH}$ as eluent. Organic fraction: 60%; ^{13}C NMR (75 MHz, CDCl_3): δ = 151.4, 150.7, 149.1, 134.1, 129.2, 128.7, 128.4, 126.0, 121.9, 120.9, 77.2, 31.8, 31.6, 31.4, 29.9, 28.9, 26.0 ppm; elemental analysis (%): found: C 44.12, H 4.36, S 3.03, N 0.12.

$\text{C}_{x_4}\text{S}_y/\text{Au}$ (**1m**): Complex **1** (0.2 g; 0.33 mmol corresponding to S/Au 1:3) was used as the gold passivating agent. Organic fraction: 37%; ^{13}C NMR (75 MHz, CDCl_3): δ = 151.4, 150.7, 149.2, 134.1, 129.2, 128.7, 128.4, 126.0, 121.9, 120.8, 77.1, 31.9, 31.6, 31.4, 29.9, 29.5, 29.2, 28.3, 26.0 ppm; elemental analysis (%): C 27.52, H 2.74, S 1.88, no N found.

$\text{C}_{x_4}\text{S}_y/\text{Au}$ (**1l**): Complex **1** (0.1 g, 0.17 mmol corresponding to S/Au 1:6) was used. Addition of the reductant solution to the reaction mixture was accomplished at room temperature. Organic fraction: 25%; ^{13}C NMR (75 MHz, CDCl_3): δ = 151.3, 150.7, 149.1, 134.1, 129.2, 128.7, 128.4, 126.0, 121.9, 120.9, 77.1, 31.8, 31.4, 29.9, 26.0 ppm; elemental analysis (%): C 18.60, H 1.92, S 1.29, N 0.10.

Nanoparticles stabilized with the bidentate calix[4]arene ligand 2

$\text{C}_{x_4}\text{S}_y/\text{Au}$ (**2s**): Complex **2** (1.2 g; 1.5 mmol corresponding to S/Au 3:1) was used as the gold passivating agent. The solid residue obtained after the centrifugation cycle required a further purification step to eliminate the large excess amount of free **2** that was contaminating the nanoparticles. A chromatographic separation was accomplished using a 9:1 mixture of $\text{CH}_2\text{Cl}_2/\text{CH}_3\text{OH}$ as eluent. During elution, the desired (**2s**) nanoparticles were visible as a dark brown band. Organic fraction: 64%; ^{13}C NMR (75 MHz, CDCl_3): δ = 153.2, 151.8, 133.4, 128.8, 128.3, 128.1, 125.2, 118.9, 77.1, 31.6, 31.4, 30.1, 29.7, 29.1, 29.0, 26.4, 22.5, 22.3 ppm; elemental analysis (%): C 48.87, H 5.19, S 5.13, N 0.05.

$\text{C}_{x_4}\text{S}_y/\text{Au}$ (**2m**): Complex **2** (0.13 g; 0.17 mmol corresponding to S/Au 1:3) was used as the gold passivating agent. Organic fraction: 46%; ^{13}C NMR (75 MHz, CDCl_3): δ = 153.1, 151.7, 133.5, 129.0, 128.8, 128.3, 128.2, 128.0, 125.2, 118.9, 76.9, 31.6, 31.4, 30.2, 29.7, 29.5, 29.1, 29.0, 28.5, 28.0, 26.3, 26.1, 22.5, 22.2 ppm; elemental analysis (%): C 32.76, H 3.69, S 3.32, no N found.

$\text{C}_{x_4}\text{S}_y/\text{Au}$ (**2l**): Complex **2** (0.07 g; 0.08 mmol corresponding to S/Au 1:6) was used as the gold passivating agent. Organic fraction: 28%; ^{13}C NMR (75 MHz, CDCl_3): δ = 153.3, 151.9, 133.5, 128.8, 128.3, 128.1, 125.2, 118.9,

77.1, 31.6, 31.4, 30.0, 29.7, 29.0, 27.2, 27.0, 26.4, 22.6, 22.2 ppm; elemental analysis (%): C 22.65, H 2.59, S 2.41, N 0.13.

Nanoparticles stabilized with the tridentate calix[6]arene ligand 3

$\text{C}_{x_6}\text{S}_y/\text{Au}$ (**3s**): Complex **3** (1.57 g; 1 mmol corresponding to S/Au 3:1) was used as the gold passivating agent. The solid residue obtained after the centrifugation cycle required a further purification step to eliminate the large excess amount of free **3** that was contaminating the nanoparticles. A chromatographic separation was accomplished using a 9:1 mixture of $\text{CH}_2\text{Cl}_2/\text{CH}_3\text{OH}$ as eluent. Organic fraction: 77%; ^{13}C NMR (75 MHz, CDCl_3): δ = 154.4, 152.0, 145.6, 145.2, 133.6, 133.2, 127.8, 123.3, 77.1, 72.9, 34.2, 31.6, 31.3, 31.1, 29.9, 29.6, 29.2, 26.4, 22.5, 22.3 ppm; elemental analysis (%): C 59.11, H 7.40, S 4.08, N 0.05.

$\text{C}_{x_6}\text{S}_y/\text{Au}$ (**3m**): Complex **3** (0.17 g; 0.1 mmol corresponding to S/Au 1:3) was used as the gold passivating agent. Organic fraction: 50%; ^{13}C NMR (75 MHz, CDCl_3): δ = 154.4, 152.0, 145.4, 145.2, 133.6, 133.2, 127.8, 123.3, 77.1, 72.9, 34.2, 31.5, 31.6, 31.0, 29.9, 29.5, 29.2, 26.5, 22.5, 22.3 ppm; elemental analysis (%): C 36.78, H 4.57, S 3.08, N 0.08.

$\text{C}_{x_6}\text{S}_y/\text{Au}$ (**3l**): Complex **3** (0.08 g; 0.055 mmol corresponding to S/Au 1:3) was used as the gold passivating agent. Organic fraction: 32%; ^{13}C NMR (75 MHz, CDCl_3): δ = 154.4, 152.0, 145.4, 145.2, 133.6, 133.2, 127.8, 123.3, 77.2, 72.9, 34.3, 31.6, 31.4, 31.1, 29.8, 29.5, 29.3, 26.4, 22.5, 22.3 ppm; elemental analysis (%): C 24.73, H 3.28, S 1.95, N 0.14.

Synthesis of calix[4]arene-stabilized Au₁₁ nanoclusters (2ex): NaBH_4 (0.033 g, 0.87 mmol) was added in small portions to a heterogeneous mixture of AuPPh_3Cl (0.43 g, 0.87 mmol) in absolute ethanol (30 mL) kept under an inert atmosphere. The resulting reaction mixture turned homogeneous within a few minutes and was stirred at room temperature for a further 2 h. After this period, the solvent was removed to dryness under reduced pressure and the solid residue taken up with dichloromethane (25 mL). The resulting solution that contained $\text{Au}_{11}(\text{PPh}_3)_7\text{Cl}_3$ nanoclusters was filtered off to remove the black suspension of colloidal gold, and the calix[4]arene **2** (0.6 g, 0.75 mmol) was added. After 24 h of stirring at room temperature, the solvent was removed to dryness under reduced pressure. The crude residue was purified following the procedure reported for the nanoparticles **2s**. Organic fraction: 62%; elemental analysis (%): C 47.04, H 4.79, S 4.49.

TEM and HAADF-STEM measurements: TEM measurements were partly carried out at CIGS of the University of Modena (Italy) using a Jeol JEM 2010 microscope. High-angle annular dark-field (HAADF) measurements were carried out at CNR-IMEM of Parma using a Jeol 2200FS field-emission microscope working at 200 kV in STEM mode. The probe size was minimized to about 0.2 nm. The size distribution of the nanoparticles was determined using ImageJ software^[38] by statistical analysis of more than 300 nanoparticles taken from at least three images for each sample.

XPS measurements: The solid compounds were homogeneously spread over a graphite tip attached to the XPS sample holder. Photoelectron spectra were acquired using a modified Omicron NanoTechnology MXPS system equipped with various photon sources and an Omicron EA-127-7 energy analyzer. The experimental conditions adopted were as follows: excitation by $\text{MgK}\alpha$ photons ($h\nu = 1253.6$ eV), generated by operating the anode at 14 kV, 16 mA. XPS atomic ratios for the investigated compounds have been estimated from experimentally determined area ratios of the relevant core lines, corrected for the corresponding theoretical atomic cross-sections and for a square-root dependence of the kinetic energies of the photoelectrons.

Acknowledgements

This work was supported by the Italian MIUR (Sistemi supramolecolari per la costruzione di macchine molecolari, conversione dell'energia, sensing e catalisi) and by Università La Sapienza. We thank CIM (Centro Interdipartimentale di Misure) “G. Casnati” of the University of Parma for NMR spectroscopic measurements.

- [1] a) J. C. Love, L. A. Estroff, J. K. Kriebel, R. G. Nuzzo, G. M. Whitesides, *Chem. Rev.* **2005**, *105*, 1103–1169; b) *Nanoparticles, From Theory to Application* (Ed.: G. Schmid), Wiley-VCH, Weinheim, **2004**; c) A. C. Templeton, M. P. Wuelfing, R. W. Murray, *Acc. Chem. Res.* **2000**, *33*, 27–36; d) G. Schmid, *Chem. Rev.* **1992**, *92*, 1709–1727.
- [2] a) *Hybrid Materials. Synthesis Characterization, and Applications* (Ed.: G. Kickelbick), Wiley-VCH, Weinheim, **2007**; b) *Functional Hybrid Materials* (Eds.: P. Gomez-Romero, C. Sanchez), Wiley-VCH, Weinheim, **2004**.
- [3] a) H. Goessmann, C. Feldmann, *Angew. Chem.* **2010**, *122*, 1402–1437; *Angew. Chem. Int. Ed.* **2010**, *49*, 1362–1395; b) *Nanoparticles: Synthesis Stabilization, Passivation, and Functionalization* (Eds.: R. Nagarajan and T. A. Hatton), ACS, Washington, **2008**; c) *Nanoparticles—Building Blocks for Nanotechnology* (Ed.: V. M. Rotello) Kluwer Academic/Plenum Publisher, New York, **2004**; d) *Colloids and Colloid Assemblies - Synthesis Modification, Organization and Utilization of Colloid Particles* (Ed.: F. Caruso), Wiley-VCH, Weinheim, **2003**.
- [4] a) R. Sardar, A. M. Funston, P. Mulvaney, R. W. Murray, *Langmuir* **2009**, *25*, 13840–13851; b) G. Schmid, U. Simon, *Chem. Commun.* **2005**, 697–710; c) M. C. Daniel, D. Astruc, *Chem. Rev.* **2004**, *104*, 293–346; d) R. Shenhar, V. M. Rotello, *Acc. Chem. Res.* **2003**, *36*, 549–561.
- [5] a) A. B. Descalzo, R. Martínez-Mañez, F. Sancenón, K. Hoffmann, K. Rurack, *Angew. Chem.* **2006**, *118*, 6068–6093; *Angew. Chem. Int. Ed.* **2006**, *45*, 5924–5948; b) A. Verma, V. M. Rotello, *Chem. Commun.* **2005**, 303–312; c) U. Drechsler, B. Erdogan, V. M. Rotello, *Chem. Eur. J.* **2004**, *10*, 5570–5579.
- [6] A. Arduini, D. Demuru, A. Pochini, A. Secchi, *Chem. Commun.* **2005**, 645–647.
- [7] T. R. Tshikhudo, D. Demuru, Z. X. Wang, M. Brust, A. Secchi, A. Arduini, A. Pochini, *Angew. Chem.* **2005**, *117*, 2973–2976; *Angew. Chem. Int. Ed.* **2005**, *44*, 2913–2916.
- [8] a) D. V. Talapin, J.-S. Lee, M. V. Kovalenko, E. V. Shevchenko, *Chem. Rev.* **2009**, *109*, 389–458; b) T. Laaksonen, V. Ruiz, P. Liljeröth, B. M. Quinn, *Chem. Soc. Rev.* **2008**, *37*, 1836–1846; c) T. H. Lee, J. I. Gonzalez, J. Zheng, R. M. Dickson, *Acc. Chem. Res.* **2005**, *38*, 534–541.
- [9] Monodispersed alkylthiol-stabilized undecagold clusters can be obtained through ligand-exchange reactions starting from the corresponding rather unstable phosphine-stabilized clusters. See, for example: a) M. F. Bertino, Z. M. Sun, R. Zhang, L. S. Wang, *J. Phys. Chem. B* **2006**, *110*, 21416–21418; b) G. H. Woehrle, J. E. Hutchison, *Inorg. Chem.* **2005**, *44*, 6149–6158; c) G. H. Woehrle, M. G. Warner, J. E. Hutchison, *J. Phys. Chem. B* **2002**, *106*, 9979–9981.
- [10] The exploitation of these properties in fields such as biology and medicine has been already documented. See, for example: a) E. Boisselier, D. Astruc, *Chem. Soc. Rev.* **2009**, *38*, 1759–1782; b) R. A. Sperling, G. P. Rivera, F. Zhang, M. Zanella, W. J. Parak, *Chem. Soc. Rev.* **2008**, *37*, 1896–1908; c) R. Wilson, *Chem. Soc. Rev.* **2008**, *37*, 2028–2045.
- [11] For a review on kinetic and mechanistic studies of the nucleation and growth of gold nanoparticles, see, for example: E. E. Finney, R. G. Finke, *J. Colloid Interface Sci.* **2008**, *317*, 351–374.
- [12] a) S. W. Chen, A. C. Templeton, R. W. Murray, *Langmuir* **2000**, *16*, 3543–3548; b) W. P. Wuelfing, A. C. Templeton, J. F. Hicks, R. W. Murray, *Anal. Chem.* **1999**, *71*, 4069–4074; c) M. J. Hostetler, J. E. Wingate, C. J. Zhong, J. E. Harris, R. W. Vachet, M. R. Clark, J. D. Londono, S. J. Green, J. J. Stokes, G. D. Wignall, G. L. Glish, M. D. Porter, N. D. Evans, R. W. Murray, *Langmuir* **1998**, *14*, 17–30.
- [13] Y. Negishi, Y. Takasugi, S. Sato, H. Yao, K. Kimura, T. Tsukuda, *J. Phys. Chem. B* **2006**, *110*, 12218–12221.
- [14] a) L.-o. Srisombat, S. Zhang, T. R. Lee, *Langmuir* **2009**, *25*, 41–46; b) B. C. Mei, E. Oh, K. Susumu, D. Farrell, T. J. Mountziaris, H. Mattoussi, *Langmuir* **2009**, *25*, 10604–10611; c) L.-o. Srisombat, J.-S. Park, S. Zhang, T. R. Lee, *Langmuir* **2008**, *24*, 7750–7754; d) S. Zhang, G. Leem, L. Srisombat, T. R. Lee, *J. Am. Chem. Soc.* **2008**, *130*, 113–120; e) K. Wojczykowski, M. P. Jutzi, I. Ennen, A. Hutten, M. Fricke, D. Volkmer, *Chem. Commun.* **2006**, 3693–3695; f) Z. Wang, B. Tan, I. Hussain, N. Schaeffer, M. F. Wyatt, M. Brust, A. I. Cooper, *Langmuir* **2006**, *22*, 885–895.
- [15] X. M. Li, M. R. de Jong, K. Inoue, S. Shinkai, J. Huskens, D. N. Reinhoudt, *J. Mater. Chem.* **2001**, *11*, 1919–1923.
- [16] See, for example: C. D. Gutsche, *Calixarenes, An Introduction*, RSC, Cambridge, **2008**.
- [17] Wei et al. have shown that resorc[4]arenes with SH groups on their upper rim can be used for the stabilization of AuNPs. See: a) A. Wei, *Chem. Commun.* **2006**, 1581–1591; b) R. Balasubramanian, B. Kim, S. L. Tripp, X. J. Wang, M. Lieberman, A. Wei, *Langmuir* **2002**, *18*, 3676–3681.
- [18] The partial functionalization of the phenolic groups present on the lower rim of calix[4]arenes enhances the preorganization of these hosts in solution of low polar solvents. Unlike the tetraalkylated ones, the aromatic cavity of mono- or dialkylated calix[4]arene derivatives has been indeed exploited as a binding site for the recognition of charged organic species. See, for example: L. Pescatori, A. Arduini, A. Pochini, A. Secchi, C. Massera, F. Ugozzoli, *Org. Biomol. Chem.* **2009**, *7*, 3698–3708.
- [19] J. D. Van Loon, A. Arduini, I. Coppi, W. Verboom, A. Pochini, R. Ungaro, S. Harkema, D. N. Reinhoudt, *J. Org. Chem.* **1990**, *55*, 5639–5646.
- [20] See, for example: a) A. Arduini, F. Calzavacca, A. Pochini, A. Secchi, *Chem. Eur. J.* **2003**, *9*, 793–799; b) J. P. M. van Duynhoven, R. G. Janssen, W. Verboom, S. M. Franken, A. Casnati, A. Pochini, R. Ungaro, J. de Mendoza, P. M. Nieto, *J. Am. Chem. Soc.* **1994**, *116*, 5814–5822.
- [21] M. Brust, M. Walker, D. Bethell, D. J. Schiffrin, R. Whyman, *J. Chem. Soc. Chem. Commun.* **1994**, 801–802.
- [22] A survey of the literature data shows that similar results were found in the synthesis of silver nanoparticles in a monophasic system (solution in DMF) by using multithiolate β -cyclodextrins (CDs) as stabilizing agents. The reduced size of the resulting nanoparticles was ascribed to a “macrocylic effect”. See: J. Liu, W. Ong, A. E. Kaifer, C. Peinador, *Langmuir* **2002**, *18*, 5981–5983.
- [23] To exclude any possible role played by the calixarene cavity in the stabilization of the small nanoparticles, as found, for instance, with resorcinarene derivatives (see ref. [17]) the synthesis of the NPs was also carried out using the 1,3-bis(*o*-undeceny)calix[4]arene **8** as ligand. This compound is structurally analogous to **2** but lacks the two alkyl chains of the anchoring points for the gold surface (see Scheme 1). As expected, the gold colloids obtained after the reduction step with NaBH₄ collapsed after the reaction workup.
- [24] For the X-ray structure of Au₂₅ nanoclusters, see: a) J. Akola, M. Walter, R. L. Whetten, H. Hakkinen, H. Gronbeck, *J. Am. Chem. Soc.* **2008**, *130*, 3756–3757; b) M. W. Heaven, A. Dass, P. S. White, K. M. Holt, R. W. Murray, *J. Am. Chem. Soc.* **2008**, *130*, 3754–3755.
- [25] The elemental analyses show that NPs stabilized with the bidentate ligand **2** that have a hypothetical empirical formula of (C₅₀H₆₆O₄S₂)₁₂Au₂₈, (C₅₀H₆₆O₄S₂)₁₀Au₂₅, or (C₅₀H₆₆O₄S₂)₆Au₁₃ would yield S/Au ratios that ranged from 0.8 to 0.92. These theoretical values are in good agreement with the calculated and mean experimental value of 0.88 (see Table 1, entry 4). Similar results can be obtained by hypothesizing the presence in the **3s** sample of NPs that have a hypothetical empirical formula ranging from (C₁₀₂H₁₅₃O₆S₃)₄Au₁₃ to (C₅₀H₆₆O₄S₂)₁₂Au₂₈.
- [26] See, for example: a) J. M. Abad, I. E. Sendroui, M. Gass, A. Bleloch, A. J. Mills, D. J. Schiffrin, *J. Am. Chem. Soc.* **2007**, *129*, 12932–12933; b) L. D. Menard, S. P. Gao, H. P. Xu, R. D. Twisten, A. S. Harper, Y. Song, G. L. Wang, A. D. Douglas, J. C. Yang, A. I. Frenkel, R. G. Nuzzo, R. W. Murray, *J. Phys. Chem. B* **2006**, *110*, 12874–12883.
- [27] The broadening of the calixarene resonances can be related to a T₂* relaxation time (which reflects the contribution of transverse relaxation time T₂ and instrumental field inhomogeneity). Short T₂* increases the resonance linewidth ($\nu_{\text{FWHM}} = 1/\pi T_2^*$; FWHM = full width at half-maximum) and is usually correlated with slow rotating

- molecules in solution. See: A. Badia, R. B. Lennox, L. Reven, *Acc. Chem. Res.* **2000**, *33*, 475–481.
- [28] G. H. Woehrle, L. O. Brown, J. E. Hutchison, *J. Am. Chem. Soc.* **2005**, *127*, 2172–2183.
- [29] a) F. Demoisson, M. Mullet, B. Humbert, *J. Colloid Interface Sci.* **2007**, *316*, 531–540; b) M. C. Bourg, A. Badia, R. B. Lennox, *J. Phys. Chem. B* **2000**, *104*, 6562–6567; c) D. G. Castner, K. Hinds, D. W. Grainger, *Langmuir* **1996**, *12*, 5083–5086.
- [30] a) S. W. Joo, S. W. Han, K. Kim, *J. Colloid Interface Sci.* **2001**, *240*, 391–399; b) S. W. Joo, S. W. Han, K. Kim, *J. Phys. Chem. B* **2000**, *104*, 6218–6224; c) S. W. Joo, S. W. Han, K. Kim, *Langmuir* **2000**, *16*, 5391–5396; d) S. W. Joo, S. W. Han, K. Kim, *J. Phys. Chem. B* **1999**, *103*, 10831–10837.
- [31] See, for example: a) R. Jin, *Nanoscale* **2010**, *2*, 343–362; b) R. L. Whetten, R. C. Price, *Science* **2007**, *318*, 407–408, and references therein.
- [32] H. Tsunoyama, N. Ichikuni, H. Sakurai, T. Tsukuda, *J. Am. Chem. Soc.* **2009**, *131*, 7086–7093.
- [33] These findings could be also useful in explaining the improved stability and reduced core size of AuNPs coated with natural molecules such as glutathione that contain an oxygen atom other than a thiol group as surface stabilizing agent. See, for example: Y. Negishi, N. K. Chaki, Y. Shichibu, R. L. Whetten, T. Tsukuda, *J. Am. Chem. Soc.* **2007**, *129*, 11322–11323.
- [34] G. W. Kabalka, M. Varma, R. S. Varma, P. C. Srivastava, F. F. Knapp, *J. Org. Chem.* **1986**, *51*, 2386–2388.
- [35] C. D. Gutsche and L.-G. Lin, *Tetrahedron* **1986**, *42*, 1633–1640.
- [36] J. de Mendoza, M. Carramolino, F. Cuevas, P. N. Nieto, P. Prados, D. N. Reinhoudt, W. Verboom, A. Casnati, R. Ungaro, *Synthesis* **1994**, 47–50.
- [37] P. Braunstein, H. Lehner, D. Matt, *Inorg. Synth.* **1990**, *27*, 218–221.
- [38] ImageJ, Image Processing and Analysis in Java. Public domain software developed at the National Institute of Health and available on the Internet from <http://rsbweb.nih.gov/ij/>.

Received: April 20, 2010
Published online: August 16, 2010